Accepted Manuscript

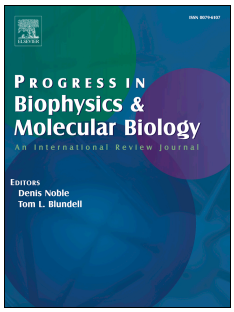

The Role of Protein-Protein Interactions in Toll-Like Receptor Function

Nils Berglund, Vasileios Kargas, Maite L. Ortiz-Suarez, Peter J. Bond

PII: S0079-6107(15)00096-6

DOI: 10.1016/j.pbiomolbio.2015.06.021

Reference: JPBM 1039

To appear in: *Progress in Biophysics and Molecular Biology*

Received Date: 17 April 2015

Revised Date: 29 June 2015

Accepted Date: 30 June 2015

Please cite this article as: Berglund, N., Kargas, V., Ortiz-Suarez, M.L., Bond, P.J., The Role of Protein-Protein Interactions in Toll-Like Receptor Function, *Progress in Biophysics and Molecular Biology* (2015), doi: 10.1016/j.pbiomolbio.2015.06.021.

The Role of Protein-Protein Interactions in Toll-Like Receptor Function

Nils Berglund[1,2], Vasileios Kargas[1,3], Maite L. Ortiz-Suarez[4], & Peter J. Bond[1,5]*

[1] Bioinformatics Institute (A*STAR), 30 Biopolis Str., #07-01 Matrix, Singapore 138671

[2] School of Chemistry, University of Southampton, Highfield, Southampton, SO17 1BJ, UK

[3] Faculty of Life Sciences, University of Manchester, Manchester, M13 9PT, UK.

[4] Centre for Molecular Science Informatics, Department of Chemistry, University of Cambridge, Lensfield Road, Cambridge CB2 1EW, UK

[5] National University of Singapore, Department of Biological Sciences, 14 Science Drive 4, Singapore 117543

* Corresponding author:
E-mail: peterjb@bii.a-star.edu.sg
Tel: +65 6478 8378

Keywords: Toll-like receptors; innate immunity; pathogen associated molecular patterns; leucine-rich repeats; transmembrane domain assembly; signaling complex formation

July 2, 2015

ABSTRACT

As part of the innate immune system, the Toll-like receptors (TLRs) represent key players in the first line of defense against invading foreign pathogens, and are also major targets for therapeutic immunomodulation. TLRs are type I transmembrane proteins composed of an ectodomain responsible for ligand binding, a single-pass transmembrane domain, and a cytoplasmic Toll/Interleukin-1 receptor (TIR) signaling domain. The ectodomains of TLRs are specialized for recognizing a wide variety of pathogen-associated molecular patterns, ranging from lipids and lipopeptides to proteins and nucleic acid fragments. The members of the TLR family are highly conserved and their ectodomains are composed of characteristic, solenoidal leucine-rich repeats (LRRs). Upon ligand binding, these rigid LRR scaffolds dimerize (or re-organize in the case of pre-formed dimers) to bring together their carboxy-terminal transmembrane and TIR domains. The latter are proposed to act as a platform for recruitment of adaptor proteins and formation of higher-order complexes, resulting in propagation of downstream signaling cascades. In this review, we discuss the protein-protein interactions critical for formation and stability of productive, ligand-bound TLR complexes. In particular, we focus on the large body of high-resolution crystallographic data now available for the ectodomains of homo- and heterodimeric TLR complexes, as well as inhibitory TLR-like receptors, and also consider computational approaches that can facilitate our understanding of the ligand-induced conformational changes associated with TLR function. We also briefly consider what is known about the protein-protein interactions involved in both TLR transmembrane domain assembly and TIR-mediated signaling complex formation in light of recent structural and biochemical data.

INTRODUCTION

The mammalian body is consistently exposed to foreign pathogens. In order to defend itself, the innate immune system provides a rapid first response to such attacks. This is achieved via recognition of various evolutionarily conserved "patterns" associated with foreign pathogenic molecules referred to as pathogen-associated molecular patterns (PAMPs) [1,2]. PAMPs are defined as being uniform within their pathogen class (i.e. virus *vs* bacteria *vs* fungi), functionally essential, and distinguishable from the host. Janeway first hypothesized in 1989 the existence of a class of receptors termed pattern recognition receptors (PRRs) in the innate immune system for PAMP recognition [3]. The PRRs would induce a signal to the host alerting it to the presence of foreign pathogens, initiating a pro-inflammatory response [1-3] that includes the expression of a large number of molecules including cytokines, chemokines, cell adhesion molecules and other immune receptors [1]. In 1997 Janeway further identified the family of PRRs called the Toll-like receptors (TLRs) [4], which remain the most extensively studied PRRs today. The importance of TLRs is highlighted by the various infectious and noninfectious disease states that can result from their dysregulation, and by their consequent extensive therapeutic targeting [5-9].

Ten functional members of the TLR family are found in the human genome (Fig 1) and each member identifies distinct PAMPs. TLRs may be distinguished by those that localize at the cell surface and recognize lipid, protein, or lipoprotein

molecules, versus those that are activated by foreign, processed nucleic acids within endosomal compartments (Table 1). The set of human TLRs recognize a broad range of ligands, including both small molecules, and large polar or nonpolar macromolecules (Table 1). TLR1, 2 and 6 respond to lipoproteins, lipopeptides and Gram-positive bacterial peptidoglycans [10,11]. TLR4 is activated mainly through lipopolysaccharide from the outer membranes of Gram-negative bacteria [12]. TLR5 is stimulated by flagellin, a protein involved in motility in many bacteria. In contrast, TLR3, 7, 8 and 9 are activated by viral pathogenic molecules [13-16], namely: TLR3, double stranded RNA [17] associated with many viruses; TLR7 and 8, single stranded RNA present in viruses such as Ebola [14-16,18]; TLR9, CpG-rich DNA, a form of DNA prevalent in viral and bacterial genomes [19].

All TLRs are type I transmembrane proteins. Each TLR is composed of an ectodomain responsible for PAMP recognition, a helical transmembrane (TM) domain, and a cytoplasmic Toll/Interleukin-1 receptor (TIR) domain [3,4,20-23]. All TLRs dimerize (TLR1-6) - or reorganize in the case of pre-formed inactive dimeric complexes (TLR7-9) - upon binding of agonistic ligands by the ectodomains. Such ligands cause dimerization by facilitating the formation of stable protein-protein interfaces between TLR chains, either directly, or via co-receptor proteins in the case of TLR4. Dimerization is proposed to initiate a signal, either through homodimerization (TLR 3, 4, 5, 8 & 9) or heterodimerization (TLR 1, 2, 6 & 10) [3,4,20-23]. The consequent rearrangements resulting from formation of the dimeric ectodomain complex are transferred via an ill-defined mechanism to the now adjacent carboxy-terminal juxtamembrane and TM helices, inducing dimerization of the cytoplasmic TIR domains. These are then proposed to act as a scaffold for the recruitment of adaptor proteins that also contain TIR domains, leading to the formation of higher-order complexes and subsequent transduction of downstream signaling [3,4,10,20-24].

The general function of TLRs is now well understood, with both physiological and non-physiological ligands identified for most, and the structural basis for ligand recognition and activation has been intensively studied for a number of these TLRs. Currently, high-resolution ligand-bound structures are available for multiple TLRs derived either from mammalian species or that are sufficiently homologous to the equivalent human TLR to derive a structural basis for function. In this review, we focus on the atomic scale protein-protein interactions that are believed to be key to TLR function. Consistent with the varying ligand specificities and cellular localization across the TLR family, each member exhibits a broad range of stabilizing dimerization interfaces, both in terms of polarity or hydrophobicity and surface area (Table 1). Crystallographic studies of TLR-ligand complexes to date have utilized truncated receptor structures, encompassing only the ectodomain involved in ligand-recognition. Thus, we necessarily focus on these associated protein-protein interactions, and the available information concerning the agonist-induced functional conformational changes and/or dynamics. We also describe those involved in the case of the unique TLR-like RP105 protein, which does not contain intracellular TIR domains but is proposed to fine-tune LPS responses via direct protein-

protein interactions with the TLR4 complex. Whilst far less is known about the interactions involved in the TM and intracellular domains, we conclude the review by briefly highlighting recent progress towards filling this gap in our knowledge, via a combination of biochemical, structural, and computational approaches.

TOLL-LIKE RECEPTOR ECTODOMAINS

The ectodomain is highly conserved across members of the TLR family, and across species [25]. TLRs are members of the leucine rich repeats (LRRs) class of proteins [26]. This prominent class is present in viruses and bacteria, as well as eukaryotic cells [27]. LRR-containing proteins play roles in a wide variety of functions, including as hormone receptors, immune receptors, tyrosine kinase receptors, and enzymes [27,28]. Despite their broad functional capacity, a general observation is that all LRRs tend to be involved in protein-protein interactions [27,29,30]. Whilst LRRs vary greatly in the number of repeated "LRR" segments and how long these segments are (~20-30 residues), the core LRR sequence motif is highly conserved, consisting of the following sequence: LxxLxLxxN (where L=Val/Leu/Ile, N= Asn/Thr/Ser/Cys, and x= any amino acid) (21, 22, 25). These repeating motifs within LRR proteins fold into bent solenoidal structures, made up of parallel β-sheets at the concave inner face, with each strand corresponding to one LRR motif, and the conserved leucine sidechains forming the hydrophobic core. The residues in the convex portion tends to adopt a more diverse range of secondary structural motifs including helices and loops [31]. In the case of the conserved asparagine residues, these help to form a continuous hydrogen-bonding network with backbone carbonyls of adjacent LRRs. The variable "x" residues are exposed to solvent and can play roles in ligand recognition. Finally, the hydrophobic core of the LRR modules at the amino- and carboxy-termini need to be buried from solvent for stability, and hence require additional disulfide bridge-containing capping modules, termed the LRRNT and LRRCT, respectively. Outside of these common features, TLRs display a number of unusual properties compared to typical LRR proteins. Thus, in contrast with most LRR ligand interaction sites, the binding sites for ligands in TLRs tend to be found on the convex sides of their solenoidal structures. Certain LRR segments in TLRs deviate from the consensus motif, resulting in specialized surfaces or pockets for ligand; in particular, TLR1, TLR2, TLR4 and TLR6 lack asparagine networks in their central region, enabling structural distortions that facilitate interactions with hydrophobic ligands including lipids and lipopeptides [20-23,32].

Upon TLR dimerization, there is very little change in the secondary structure or conformation of the individual chains, demonstrating the rigidity of the LRR motifs [31]. Thus, the overall shape of each ligand-bound ectodomain TLR dimer is strikingly similar, forming a characteristic "m" shaped structure with the carboxy-termini tails in the center of the complex, enabling juxtaposition of the intracellular TIR domains. On the other hand, whilst TLR1, TLR2, TLR6 and TLR10 are similar in size, with 20 LRR repeats, TLR3, TLR4 and TLR5 have 25, 23 and 22 LRRs respectively, whilst TLR7, TLR8 and TLR9 are bigger still with 27 LRRs each [33]. The number of LRRs involved in each TLR-TLR interface differs greatly between family members and does not necessarily correlate with

the size of the proteins (Table 1). The largest TLR ectodomains, TLR8 and TLR9 (and probably TLR7), utilize 9-10 LRRs at their dimer interface. The smaller ectodomains of TLR1, TLR2 and TLR6 (and probably TLR10) involve 4-5 LRRs at the dimer interface, whilst four LRRs are involved in the dimer interface of TLR4, and just 1-2 LRRs in the case of TLR3 and TLR5.

In the following section, we focus on the ectodomains of individual TLR homo- and hetero-dimers, and highlight key features of their associated protein-protein interactions that facilitate ligand recognition, dimerization, and downstream signaling.

TLR1-TLR2 and TLR2-TLR6 Heterodimers

TLR2 is a unique member of the TLR family in that it can dimerize with both TLR1 and TLR6; the resultant heterodimers are respectively specific for either tri-acylated or di-acylated bacterial lipopeptides and lipoproteins. The tri-acylated lipopeptides are often associated with Gram negative bacteria [10,24,34,35], whereas their di-acylated counterparts [11] are predominantly found in Gram positive bacteria. There is significant heterogeneity in the structure and length of these lipopeptides *in vivo*. The structural basis for ligand recognition has been facilitated by the use of synthetic lipopeptides that mimic their bacterial counterparts, such as di-acylated Pam_2CSK_4 and tri-acylated Pam_3CSK_4.

The crystal structure of human TLR2-TLR1 heterodimers bound to Pam_3CSK_4 revealed that two acyl chains insert into the internal binding pocket on TLR2, a crevice formed between LRR11 and LRR12, extending internally to LRR9, whilst the final acyl chain inserts into a smaller binding channel present in the same region of TLR1. The ligand essentially bridges the two proteins, creating a coherent dimer interface [10]. This interface is stabilized through a hydrophobic core at the center, surrounded by hydrophilic residues forming hydrogen bonds and ionic interactions. The hydrophobic "patch" is composed of P315', Y320', V311', V339' and L359' on TLR1 (where an apostrophe corresponds to TLR1) and Y323, L324, F322, P352, Y376, L350, F349, L371 and V373 on TLR2 [10]. Polymorphic variants of TLR1 without P315' present in the interfacial hydrophobic core exhibit inhibited signaling behavior [36]. The hydrophilic region bordering the hydrophobic patch forms hydrogen bonds including K385'-N345, T361'/T363'-K347, R337'-E375, and Q383'-H398, and ionic interactions are formed via E321'-H318/R321, E366'-R321, K385'-E369, R337'-E374, and D310'-K378 [10]. These regions are highly conserved across species, consistent with an identity between mouse and human sequences of 73% and 68% for TLR1 and TLR2, respectively [10]. Minor differences in sequence account for some variations in specificity between species. For instance, mouse TLR2 has a more compact binding pocket than the human equivalent [37], whilst the equine TLR1/TLR2 heterodimer has different affinity to Pam_3CSK_4 than the human dimer [38]. The peptide portion of the lipopeptide forms additional hydrogen bonds with the TLR chains to stabilize the bound conformation [10].

TLR1 and TLR6 are highly homologous, sharing 56% sequence identity in mice [11]. Differences in sequence around LRR9 to LRR12 in TLR6 compared to TLR1

lead to a change in specificity, though they still activate the same pathway [11,39]. Unlike the dimerization interface in the TLR1-TLR2 complex that is mediated by the binding cavities present between LRR9-12 on TLR1, the crystal structure of mouse TLR2-TLR6 in the presence of Pam_2CSK_4 revealed that dimerization is mediated by the surface exposed amino acids between LRR11-14 (Fig 1B). In the latter complex, TLR2 still binds the two acyl tails within the internal binding cavity between LRR11 and LRR12 [11]. However, in TLR6, differences in the sequence compared to TLR1 results in a structural change such that F319', L324' and Y325' move into the acyl chain binding channel present in TLR1, and effectively truncate it [11]. Much like TLR1-TLR2, the TLR2-TLR6 interface is composed of a central hydrophobic core surrounded by hydrophilic residues that form hydrogen bonds and ionic interactions. Residues including F317', L318', Y325', P342', I344', V347' and V364' constitute the hydrophobic "patch" on TLR6, highly conserved between species, and interact with F322, Y323, L324, F349, L350, L371, V373 and Y376 on TLR2. Hydrogen bonds formed at this interface include N314'-E375, P342'-Y376, Q362'-R400 and T366'-K347, along with salt bridges including H311'-E375, K313'-E375, D340'-R400/R404, D367'-H318/K347 and K390'-E369 [11]; unsurprisingly, many of the interacting residues from TLR2 are also involved in the TLR1 complex. Hydrogen bonds between ligand and loops of LRR11 also contribute to the stability of the complex by bridging TLR2 and TLR6, locking the conformation of the residues within the hydrophobic core into position [11]. Despite the reduced number of internalized acyl tails at the dimer interface, stable heterodimers form between TLR2 and TLR6 suggesting that the additional protein-protein interactions compensate for the reduction in ligand-protein interactions. This is in accordance with the observation that there is an 80% increase in the size of the hydrophobic "patch" of TLR6 compared to TLR1 [11].

TLR10 Heterodimer

TLR10 is believed to form heterodimers with TLR2 in a similar mode to TLR1, as TLR10 exhibits conservation of key residues at the dimerization interface and a lipopeptide binding channel, though lipopeptide binding has not yet been shown to induce signaling [40]. No data is so far available to confirm a precise agonist for TLR10, and no crystal structure is available for the ectodomain, though it has been shown to be involved in the response to viral infections, particularly influenza A [41]. Homology modeling studies indicated that like TLR1-TLR2, the TLR10-TLR2 complex is likely to have a large hydrophobic core surrounded by hydrophilic residues stabilizing the dimer interface [40]. The residues predicted to be in the hydrophobic core are L342', Y320', Y313', V311', P339' and I359' on TLR10, and Y323, L324, F322, P352, Y376, L350, F349, L371 and V373 on TLR2. This hydrophobic core resembles that of TLR1-TLR2 with residues being conserved (Y320 and V311) or conservatively preserved (L359/I359' and V339/P339'). Hydrogen bonds stabilizing the interface may include: K383'-E369/N345, E385'-N345, T361'-K347, E363'-K347, Q337'-E375 and N357'-H398. In this region, a number of residues are conserved between TLR1 and TLR10 (K385/K383' or E385', T361/T361', T363/E363', R337/Q337') [40]. Finally, ionic interactions at the interface are predicted to form between E363'-H318/R321/K347, D317'-R321, D362'-K347, E385'-K347, K383'-E369, R310'-E374/E375 and H308-E375. Only E321/D317', E366/E363' and K385/K383' are

conserved in this region [40]. Mutational studies performed at the hydrophobic core of TLR10 revealed that substitution of T320', P339' or I359' with polar or charged residues dramatically reduces the binding of Pam_3CSK_4, which is capable of binding to TLR10 but not activating it [40]. Whilst TLR1 still retains most of its function in a Y320 mutant, the same mutation in TLR10 leads to a significant loss of binding ability. These mutational studies suggest that though similar in overall structure, TLR10 has subtle differences at its dimer interface that are likely to be the root of the difference in specificity between TLR1 and TLR10 [40]. Until a crystal structure is available and a TLR10 agonist identified, these results remain to be verified.

TLR5 Homodimer

TLR5 is activated by monomeric flagellin, a part of the tail-like portion of the protein flagellum that is responsible for bacterial motility [42]. There is still no crystal structure for mammalian TLR5, but a structure for zebrafish TLR5 as part of a variable lymphocyte receptor (VLR) hybrid has been determined (Fig 1E). In addition, an electron microscopy structure was solved at 26 Å resolution for full length human TLR5 [43]. These studies revealed that TLR5 forms an asymmetric homodimer via ectodomain interactions [42-46]. It is also suspected that TLR5 may dimerize in the absence of ligand [44], though conflicting structural evidence suggests that TLR5 may first heterodimerize with flagellin before forming the TLR homodimeric complex [43]. TLR5 contains glycosylation sites on its surface but retains a glycosylation free face where the TLR5-TLR5 dimer interface is located, along with the ligand binding site. The primary ligand binding site is located on the amino-terminal portion of TLR5 between LRRNT-LRR10, and is split into two interfaces, A and B. Interface A is present between the concave and ascending region of the glycosylation-free face of LRRNT-LRR6, while interface B is present on the ascending glycosylation free face between LRR7 to LRR10. The secondary interface contains the dimerization interface of TLR5-TLR5, as well as a secondary ligand-binding interface for flagellin with the alternate TLR5 [43]. The secondary dimerization interface is maintained through hydrophobic interactions between three hydrophobic residues in the zebrafish structure, namely F273, F351 and H375. These residues are highly conserved across species, with the only sequence difference being the replacement of H375 by leucine in human, bovine, mouse, and chicken. There are also two sets of hydrogen bonds stabilising the interface, which are formed between R377-N350 and R377-Y373 [43]. Once a crystal structure is solved for human TLR5, these observations may be further verified.

TLR3 Homodimer

TLR3 is found in endosomes and dimerizes upon exposure to dsRNA molecules, which are PAMPs associated with a diverse range of viruses. Like TLR5, it maintains one glycosylation-free face where ligand binding occurs and where the dimerization interface is present [13,17] (Fig 1C). The electrostatic binding surface of TLR3 is basic, consistent with the overwhelmingly negatively charged nature of dsRNA, and includes two basic "patches" located around LRR12 and in the amino-terminal region around LRR3 [17]. Unlike the latter site, LRR12 has an extended LRR sequence composed of 33 residues, creating an insertion following the β-strand segment, which leads to a protrusion in the glycosylation free face

that is of functional significance [13,17]. The TLR3 homodimerization interface is located at the carboxy-terminus around LRR20, also on the glycosylation free face; this region contains the densest cluster of conserved, surface exposed residues across species. Similarly to TLR2-associated heterodimers, surface exposed residues rather than internal binding cavities mediate TLR3 homodimerization [17]. Distinct from the previously mentioned TLRs however, the TLR3-TLR3 interface is largely hydrophilic, stabilized mostly by ionic interactions and hydrogen bonds. Ionic interactions are formed between E442-K467 and K547-D575, and further stabilization of the interface is achieved either through direct hydrogen bonds with the opposite TLR3 chain or through bridging waters. Direct intermolecular hydrogen bonds include the following: E442-K467, N517-N517, N541-N541, R544-N620/N596, K547-D575, N597-N597 and N597-R544 [17]. A relatively limited number of intermolecular hydrophobic interactions are involved, formed via A549, P551 and L621 on LRR20, which like LRR12 has an extended LRR sequence with a protrusion on the convex portion of the carboxy-terminal region [13,17].

TLR7, TLR8, and TLR9 Homodimers

TLR7, TLR8, and TLR9 are also found in acidified endosomes, and bind nucleic acid fragments. Unlike other TLRs, they are synthesized as pre-formed dimers in the absence of an agonist. TLR7 and TLR8 bind single stranded RNA, whilst TLR9 recognizes unmethylated CpG DNA, a form of DNA rarely found in vertebrates but commonly associated with viral and bacterial genomes [15,19] (Figs 1F, G). TLR7 and TLR8 are also activated by certain small molecules with immunomodulatory properties. Recent crystal structures have revealed how TLR8 [14] and TLR9 [19] form homodimers without the presence of ligands, consistent with the large buried area formed between chains. Whilst no crystal structure is available for TLR7, the 43% sequence identity to TLR8 suggests that the structure of the dimeric complex should be conserved [16,18]. Due to the large size of each TLR8 ectodomain (>800 residues), and its almost completely circular shape, the dimerization interface is very large (2,150 $Å^2$ in the ligand bound form versus 1,290 $Å^2$ in the unliganded state). Hence, unlike TLRs 1-6, none of whose dimerization interfaces exceed 800 $Å^2$ in buried surface area (Table 1), mutation of a single residue within the TLR8 interface is unlikely to abrogate dimer formation, though it may affect signaling [16,18]. Likewise, the dimerization interface in the TLR9 homodimer is extensive (>40 residues) [19]. Residues involved in the TLR9 interface are found in the carboxy-terminal LRRs (LRR20 to LRRCT) as well as LRR18, LRR11, LRR8, LRR5 and LRR2 and are highly conserved across species [19], whilst ligand binding is mediated through surface exposed residues between LRRNT to LRR10 on the primary TLR9 chain and the carboxy-terminal segment LRR20 to LRR22 on the alternate TLR9.

Key insights into the mechanism of signaling by TLRs were provided by the crystal structures of TLR8 in the liganded versus unliganded state [19] (Figs 2A, B). In the case of the ligand-free, preformed TLR8 dimer, the symmetric TLR8/TLR8 interface spans between LRR8 to LRR18 [16,18]. The interface is maintained by a large number of hydrogen bonds between LRR8, LRR14 to LRR15 and LRR18, and by a hydrophobic core consisting of F261, V378, P432, Y348, Y353, F405, F494, F495, Y567, and F568, that are distributed around

LRR8, LRR11 to LRR15, and LRR18 [18]. Upon binding of small molecule, imidazoquinoline-based ligands that bridge the chains in a hydrophobic pocket around LRR11 [18], the complex undergoes both local and global conformational changes.

Local structural changes occur in the loop structures of LRR8 and LRR17 to LRR20, coupled with large-scale conformational changes at the TLR dimer interface, causing the two ectodomain chains to rotate with respect to each other. This results in a shift in a dimerization interface that encompasses LRR5, LRR8 and LRR14 to LRR20, and allows the bound ligand to form strong polar interactions with the highly conserved D543 on LRR17. From LRR14 to LRR20, additional intermolecular hydrogen bonds form between N491-R541, A514-R541 and E427-H566 and new van der Waals contacts are formed between F494-F494 and S516-S516 [18]. In the peripheral region (LRR11, LRR8 and LRR5), extensive van der Waals contacts and hydrogen bonds further stabilize the new dimerization interface. Strikingly, the rearrangement of the TLR8 complex also causes the ectodomains to tilt (Figs 2A, B), bringing their carboxy-terminal ends into closer proximity, from ~5 nm to ~3 nm separation. It is speculated that this would enable the intracellular TIR domains to dimerize in the full-length protein, thus facilitating formation of a platform for recruitment of adaptor proteins to initiate downstream signaling [14-16,18].

STRUCTURE AND DYNAMICS OF TLR4/MD-2

The TLR4 signaling pathway is well studied, not least because of its importance in the development of anti-septic drugs and vaccine adjuvants. This is due to the nature of its main PAMP, lipopolysaccharide (LPS), a glycolipid from Gram-negative bacterial outer membranes [12,47-54]. Only small amounts of LPS are required to stimulate the TLR4 pathway and hence alert the immune system to invading pathogens, and overstimulation of this pathway can lead to sepsis. Septic shock remains the primary killer in intensive care units, with a 30% mortality rate, and millions of deaths worldwide every year [6-8]. Identifying drugs that inhibit TLR4 complex dimerization and hence sepsis is thus of great interest. LPS molecules can be sub-divided into an oligosaccharide core and variable O antigen region, plus a hydrophobic anchor containing multiple acyl tails and a phosphorylated glucosamine headgroup termed lipid A [55]. Lipid A is the main bioactive component of LPS [12,49], but subtle variations in its structure can have a major impact on stimulation of the TLR4 pathway. For example, hexa-acylated, bi-phosphorylated lipid A from *E. coli* is a potent agonist of TLR4 in all known species, whereas its biosynthetic intermediate, tetra-acylated lipid IVa, is an antagonist in humans (but an agonist in mice and horses) [56].

The TLR4 ectodomain structure resembles that of other TLR family members in the presence of both agonists [57] or antagonists [12,58] but its dimerization state is regulated in cooperation with a co-receptor protein, MD-2 (myeloid differentiation factor 2), to form a productive $(TLR4/MD\text{-}2)_2$ heterotetrameric complex [12] (Fig 1D). MD-2 adopts an immunoglobulin-like β-cup fold whose hydrophobic interior is specialized for binding lipid molecules. LPS is transferred to MD-2 via a specialized relay of proteins *in vivo* including LPS-binding protein

(LBP) and CD14, but the binding of agonistic LPS to MD-2 is the key factor in determining TLR4 signaling, since MD-2 binds to the amino-terminal region of TLR4 and mediates active complex formation [48-53,59-61].

In the heterotetrameric receptor complex, the TLR4-TLR4 interface is located in the carboxy-terminal portion of the proteins between LRR13 to LRR20 (Table 1). This region is predominantly stabilized by intermolecular hydrogen bonding with interactions observed between S386-N365', S386-S386', N433-N433', Q507-Q507', K435-N433' and N486-Q507', where an apostrophe corresponds to the second TLR4 chain [12,48,57]. The only hydrophobic contacts believed to be involved in stabilizing the interface in this region are symmetric V411/V411' interactions, though the sidechains of F533 present on LRR22 below this interface are angled towards each other and may also be involved [57]. Interestingly, a number of histidine residues are present in and around the dimerization interface and are highly conserved between species (H431, H458 and H555 at the interface, and H456 and H529 adjacent)[47]. Changes in the ionization state of these residues have been proposed to be the source of TLR4's unique ability to activate different downstream signals at the cell surface versus in acidic endosomes, via pH-dependent conformational changes within the dimeric TLR4 complex [47].

The interactions between TLR4 and MD-2 may be broken up into two main zones (Fig 1D). A primary interaction site exists between the MD-2 protein and the concave surface of its complimentary TLR4, which is present even in the presence of antagonists [12,58] resulting in a buried area between TLR4 and MD-2 of ~800 $Å^2$ and stabilization of the signaling-inactive TLR4/MD-2 heterodimeric complex. The secondary interaction site, which exists only in the presence of agonists, is formed between the same MD-2 chain and the convex surface of the alternate TLR4'/MD-2' complex [57], burying ~600 $Å^2$ between the TLR4' chain and MD-2, thus stabilizing the $(TLR4/MD\text{-}2)_2$ heterotetramer (Fig 3A). At the primary interaction site, protein-protein interactions between MD-2 and TLR4 (with MD-2 residues quoted first) include a number of ionic bonds formed between R106-D209, D99-R289, R68-E42 and K109-D60/84, along with hydrogen bonds formed between S103-E266/N265, D101-R264/S317, S98-R289 and D99-R289 [12,48,57]. Protein–protein interactions at the secondary interface between MD-2 and TLR4' involve ionic interactions between K125-E422 and R90-E439, hydrogen bonds between G123-S416, K125-N417 and R90-Q436 [48,57], along with an extensive set of ligand-dependent hydrophobic contacts, as discussed below.

Comparison of structures in the presence and absence of an agonist reveal subtle conformational changes in a loop within MD-2 containing the F126 residue. In the LPS-bound $(TLR4/MD\text{-}2)_2$ complex, F126 is located near to the secondary dimerization site but is oriented inside the MD-2 binding cavity (Fig 3A), interacting with L54, Y131, I124 and the bound lipid tail [57]. In contrast, in agonist-free crystal structures of the TLR4/MD-2 heterodimer, this loop adopts different conformations in which the phenylalanine sidechain is solvent exposed (Fig 3B). Recently, molecular simulation approaches revealed that the β-cup fold of MD-2 is extremely dynamic and can undergo "clamshell-like" motions [48],

similarly to other distantly related lipid-binding proteins [62], allowing it to adapt to the size and shape of different ligands bound within its hydrophobic cavity. Importantly, this dynamic adaptation was shown to be allosterically coupled to the F126 loop, and to determine the stability of the active receptor complex. Thus, in the presence of a bound agonist, F126 remains within the MD-2 cavity (Fig 3A), enabling MD-2 residues including I80, V82, and L87 and an exposed lipid tail to form extensive hydrophobic contacts with TLR4' residues at the secondary dimerization interface; these include F440', L444', and F463', supported by a salt bridge between E422' and K125 on MD-2 [48,57]. However, in the presence of antagonists or in the ligand-free state, F126 was observed to spontaneously reorient and exit the MD-2 cavity, leading to a disruption of the hydrophobic cluster at the secondary dimerization interface and a loss of as much as ~400 $Å^2$ of buried surface area between TLR4' and MD-2 [48,53] (Fig 3B). Over longer timescales, it is expected that such disruption would lead to a loss of TLR4 dimerization and consequently separation of the TIR juxtaposition necessary for downstream signaling. Indeed, analysis of the dominant simulated motions associated with loss of agonist indicates that the carboxy-termini of the TLR4 ectodomains exhibit lateral fluctuations associated with chain separation (Fig 2C, D), not unlike the conformational changes observed in crystal structures of the pre-formed TLR8 dimer upon ligand unbinding (Fig 2A, B). The idea that F126 acts as a molecular switch to determine the key protein-protein interface for TLR4 dimerization is supported by mutational studies, which reveal that F126 and nearby residues in this loop do not prevent lipid ligand binding but interfere with signaling [12,48,53,57], and by NMR studies using metabolically labeled endotoxin which demonstrated that this loop reorients upon ligand binding [53].

RP105 AND REGULATION OF TLR4

RP105 (Radioprotective 105 kDa, also known as CD180) is a type I TM protein that shares the characteristic solenoidal LRR ectodomain structure observed in other TLRs. Analogous to TLR4, RP105 requires a co-receptor for dimerization and cell-surface expression: the MD-2-related protein MD-1 [63-65] with which it forms a 2:2 heterotetramer, including two copies each of RP105 and MD-1 (Fig 4A). The shared architecture and sequence similarity between the two receptors (~30 % for RP105 and TLR4) suggest a common physiological role, and the RP105/MD-1 complex is believed to be a regulator of the LPS-induced TLR4/MD-2 signaling response. This receptor has been reported to fine-tune TLR4 pathways, and studies also suggest that it may regulate TLR2-induced macrophage responses to *M. tuberculosis* lipoproteins [66]. RP105/MD-1 stimulation is primarily mediated and restricted to B cells, and leads to B cell proliferation [67,68], activation, and differentiation via a T cell-independent pathway [69], all of which are modulated by MyD88-dependent TLR signals [70].

To date, the human, bovine, and mouse forms of RP105-MD-1 complex have been crystallized [71,72], and these share ~70 % sequence identity with one another. Unlike the typical tail-to-tail arrangement of juxtaposing carboxy-termini in TLRs, in all available structures the RP105 the units are arranged in a novel "m-shaped" head-to-head fashion, placing the amino-terminal regions at the center of the complex. Tail-to-tail assemblies facilitate the interaction of the TIR

domains in TLRs. However, RP105 lacks the TIR receptor domain required to transduce signals into the cytoplasm [21], and instead contains only an intracellular tail of 6-11 residues [64]. The heterotetrameric $(RP105/MD\text{-}1)_2$ assembly has two partially overlapping interaction interfaces. RP105 and MD-1 form a primary interface, and then homodimerize into a 2:2 complex using a secondary dimerization interface, by analogy with TLR4.

The primary interface in RP105/MD-1 is divided into three discontinuous regions corresponding to interfaces A, B, and C. Interfaces A and B involve protein-only contacts of the amino-terminal and central domains of RP105 and MD-1, and these are mostly conserved in TLR4/MD-2. On interface A, the conserved polar MD-1 residues form extensive contacts with RP105 residues on the concave side of LRRNT and LRR1 to LRR6. These include (with MD-1 residues quoted first) the salt bridge K113-E40, and hydrogen bonds between R72-N41, G114-R86, R111-S158, and E115-Q134.

Additionally, residues K116, G117 and E118 on MD-1 (and similarly MD-2) associate with F62, D83, and R86 on RP105 (and TLR4), all of which are fully conserved across species [71]. A small patch of hydrophobic interactions is also present, formed by the spatially adjacent residues K113, G114, and E115 of MD-1 and T85, T109, T113 of RP105 [72]. Interface B is formed by residues on LRR9-LRR13 on RP105, and eleven MD-1 ones. The major contribution here comes from the protruding loop of LRR9 forming three backbone hydrogen bonds on S107-D257 and K105-E256. The charge complementarity observed in human TLR4/MD-2 binding is not as pronounced in human RP105/MD-1, with only one salt bridge being formed, E40-K113 [72]. Overall, there are fewer protein-protein interactions that contribute to the primary interface in human RP105 than there are in TLR4. Nonetheless, this primary interface has a unique additional region C, created by an N402-linked glycan on the concave face of LRR15. The well-ordered glycan interacts extensively with RP105 and MD-1 through polar interactions in the crystal structure, though expression of a non-glycosylated bovine RP105 leads to relatively stable complexes [72], and molecular simulations indicate this this complex is not disrupted in the absence of the glycan moiety (unpublished data).

The dimerization interface in RP105 is made up of two regions: an RP105'/MD-1 (α) interface and an RP105/RP105' (β) one, where an apostrophe corresponds to the second RP105 chain. Interface α is made up of 19 hydrophobic residues from RP105 (W91, I114, F115, F142, highly conserved in all species) that are stacked against a flat face of beta sheets on MD-1 (G49, G68). Nearby polar interactions support the hydrophobic regions (with MD-1 residues quoted first), including: R66-E141, T28-E94, and Q116- S138, and some π-stacking between F142-Y118. The smaller dimerization interface β is symmetric and hydrophobic with interactions between H186-H186', and a polar pairing between S162-K212'.

Despite some controversy on its reported cell-dependent dichotomous effect on TLR4 signaling, it is thought that in antigen-presenting cells the RP105 complex down-regulates LPS responses by direct interaction with TLR4, preventing dimerization from occurring [73,74]. It has been suggested that this may be

achieved as a result of the MD-1 bound RP105 carboxy-terminal region replacing the equivalent homodimerization interface of the TLR4/MD-2 receptor complex [71,72] (Fig 4B). This would involve polar interactions between residues R431, H433, E383 of RP105 and K453, R460, Q436 and E439 of TRL4 without any major structural reconfiguration. Whilst this is an attractive model for the apparent inhibitory behavior of the LPS-induced TLR4 response by RP105, confirmation awaits high-resolution structural data of the complete inhibitory complex.

TLR TRANSMEMBRANE DOMAINS

The TM domains (TMDs) of many membrane proteins are associated with their activation, assembly and regulation [75-77]**.** The functional significance of TMDs and their mechanisms of assembly have previously been demonstrated for many membrane proteins including integrins, receptor tyrosine kinases and G-protein coupled receptors [78-80]. Several biochemical studies have emphasized the functional relevance of TMD interactions and their regulation [81-84] in the TLR family. Recently, the ToxR assay was used within *E. coli* membranes to study the intrinsic capacity for homo- and hetero-dimerization of the isolated TMDs from all human TLRs [75]. The TLR TMD segments were thus expressed as a chimeric protein, fused to an extracellular maltose-binding protein that orients the construct to the periplasm, along with a cytoplasmic cholera toxin transcriptional activation domain (ToxR). Upon TMD oligomerization, the dimeric ToxR domains bind to their promoter, leading to expression of the β-galactosidase reporter [85-87]. All human TLR TMD constructs exhibited strong homotypic interactions, whilst TLR2 formed stable heterodimers only with their associated subfamily members, TLR1, TLR6 and TLR10 [75], consistent with their biologically relevant roles in ligand recognition discussed above, and with their high sequence identities of ~50-90%. Further biochemical and biophysical assays showed that exogenous synthetic peptides of mouse TLR2 and TLR6 TMDs, expressed in macrophages, affect TLR2 activation by inhibiting TNF-α secretion upon stimulation by lipoteichoic acid, a TLR2/6 activator from Gram-positive bacteria [5]. These studies confirmed heterodimerization and strong associated heterotypic interactions between the TLR2 and TLR6 TMDs. Moreover, *in vivo* studies have demonstrated the potential for therapeutic targeting by TMDs, by showing that these peptide constructs could inhibit TLR2 activation, reducing lethal inflammation in mice [5].

As pointed out by Shai and co-workers [22], several amino acid motifs known to be involved in self-assembly and stability of other TM helix-helix interactions are present in the TLR TMDs, such as Small-xxx-Small (TLR2/7/9/10), aromatic-xx-aromatic (TLR5/8), and polar-xx-polar (TLR1/5/6) motifs, along with the general presence of multiple TM polar residues that may place a possible functional role in membrane assembly and transmembrane receptor function. A recent solution NMR spectroscopy study revealed the conformations of both dimeric and trimeric assemblies of the TLR3 TMDs in dodecyl-phosphocholine (DPC) detergent micelle environments, providing the first atomic-resolution structural information for the oligomerization of TLR TMDs [88]. Both the homodimer and homotrimer were shown to adopt α-helical conformations within detergent micelles [88], consistent with circular dichroism data measured

for other members of the TLR family [5,75]. In the dimeric conformation, the protein-protein interaction interface involved symmetrical contacts between residues F706, T710, L714 and F718 [88] (Fig 5A). The aromatic rings of F706 and F718 in particular make van-der-Waals contacts across the interface with the potential for stacking interactions. In the case of the trimeric structure, two distinct contact surfaces could be identified in addition to the symmetrical dimerization interface, including F705, N709, L713 and I717 on one side of the TM helix, and I708, I712 and F716 on the other [88]. Whilst the biological relevance of the trimer may be questionable, since there is no evidence for such functional oligomerization in TLRs, the observed contact surfaces are in agreement with a model for the full-length TLR3 receptor in the active state proposed by Davies and co-workers [89], suggesting that there may be multiple TM interfaces associated with different functional states of the TLR3 receptors. The oligomers and associated TM helix-helix interactions were observed to be more stable at low pH, possibly due to intermolecular H724-E726 contacts between the helices [90]. The dimerization and trimerization free energies measured for TLR3 [88] were slightly more stable than those of other TM domains such as ErbB3 [91] and ErbB4 [92], but much weaker than the archetypal transmembrane homodimer, glycophorin A (GpA), whose TMD contains the GXXXG motif [93,94].

Whilst the NMR structure provides important structural insights into the assembly of the TLR3 TMDs within detergent micelles, the high-resolution interaction mode of these helices within phospholipid bilayers remains undefined. This is important, since solution and solid-state NMR studies of the GpA TMDs revealed homodimeric structures within both detergent micelles and lipid membrane environments respectively, but an altered crossing angle and difference in interfacial packing arrangement was observed [95,96]. A molecular simulation approach may be taken to help resolve these differences. As demonstrated using both atomically-detailed [97] and simplified, coarse-grained simulations [98] of GpA, different converged TM dimeric structures result depending upon the local environment. Thus, a significant relative rotation and crossing angle of the two helices was observed when comparing GpA dynamics within detergent micelles versus phospholipid bilayers, and the TMDs were observed to sample a significantly larger range of crossing angles in the micelle environment [97]. By analogy, similar simulation studies have been undertaken for the TLR3 TM homodimer within a palmitoyl-oleyl-phosphatidylcholine (POPC) lipid bilayer (unpublished data), based on the dimeric NMR structure (Fig 5B). Preliminary results from 200 ns all-atom simulations [88] revealed a significantly smaller crossing angle (~30^{o}) between the helices compared to the NMR structure (~60^{o}), and a consistent switch in the interaction interface (Fig 5C). Thus, the sidechains of the weakly interacting F706 as well as those of T710, which do not take part in polar intermolecular contacts in the NMR structure but instead form intramolecular hydrogen-bonds [88], were observed to rotate away from the interaction interface. This was compensated by improved intermolecular stacking interactions between F718 and van-der-Waals contacts between L722, maintaining a favorable buried surface area at the protein-protein oligomerization surface and an optimized transmembrane configuration within the phospholipid bilayer environment (Fig 5C). Confirmation of whether

similar principles apply to other TMD members of the TLR family awaits further structural and computational studies.

DOMAINS ASSOCIATED WITH DOWNSTREAM SIGNALING

TIR domains brought together by dimerization act as scaffolds for downstream adaptor proteins for subsequent propagation of signal cascades [5]. Adaptor proteins also contain TIR domains and associate with receptor dimers through TIR/TIR interactions. TIR domain containing proteins include not only receptors but also signaling-adaptor proteins. Heterotypic TIR-TIR interactions between receptors and adaptors thus enable formation of higher-order complexes, which eventually lead to activation of key transcription factors and production of cytokines [21,99]. Thus, the MAL (or TIRAP) adaptor bridges MyD88 to receptor TIR domains, whilst TRAM likewise bridges TRIF to receptors, to facilitate alternate downstream signaling pathways. The MyD88 pathway is associated with all TLRs except TLR3, which uses TRIF alone, whilst TLR2 and TLR4 can signal through both MyD88 and TRIF.

A number of crystallographic structures are available for both receptor and adaptor TIR domains, providing useful information concerning potential interaction interfaces and rationalizing conservation patterns and/or mutations that affect TIR domain functionality [100-102]. Unfortunately, there is presently limited high-resolution information on the homotypic and heterotypic interactions required for the binding of adaptor TIRs to those of the TLRs. This may be because isolated TIR domains do not form stable multimers when detached from their full-length construct [102], whilst TIR-TIR domain interactions appear to be weak and transient, suggesting stable dimerization may only occur in the larger context of multivalent macromolecular complexes [99].

Structures of TIR domains from TLR1, TLR2, TLR6, TLR10, MyD88, and MAL indicate that all share a common α/β architecture comprising four or five parallel β-strands (βA-βE) surrounded by five α-helices (αA-αD) [102]. Early crystal structures of isolated TLR1 and TLR2 TIR domains revealed a large conserved surface patch crucial for receptor signaling, which contains a key region, the BB loop (which connects the αB-helix with the βB-strand) exposed on the surface. Mutation of a proline residue (P681 in TLR2) to histidine within the BB loop that is conserved across most mammalian TLRs (except TLR3) disrupts signal transduction [102-105], indicating that the conserved patch mediates interactions with downstream adaptor molecules. The importance of the BB loop in dimerization is supported by several crystallographic studies of TLR TIR domains [100,101,106], and by BB loop peptide decoys which inhibit TLR signalling [107], paving the way for the design of specific antagonists against certain downstream TLR pathways [108] [109]. In addition to the BB loop, the DD loop (connecting the αD helix to the βD strand) has been shown to be important for signaling, and may mediate heterotypic interactions with the BB loop on partner TIR domains [24].

In contrast to TLR2 [110], structures of TLR6 [100] and TLR10 [101] TIR domains revealed two-fold symmetrical homodimeric interfaces; in the case of

TLR6, the dimeric interface was formed via mutual interactions between the CD loop, DD loop, and αC helix, whereas for TLR10, this interface was formed mainly by the αC helices plus BB loops. It is thus possible that there is no single universal dimerization interface for TIR-TIR interactions, and it is also important to note that the length and conformation of loops across the TIR domain family vary significantly. Nevertheless, models for heterotypic TIR signalling complexes have been proposed on the basis of the various available crystallographic and biochemical data. One notable study combined information from the X-ray structure of homodimeric TLR10 TIR [101] with protein docking to model the receptor-adaptor TIR complex for TLR4. This placed the BB loop forming homotypic interactions between receptor TIR domains, with the TIR domains of TRAM and MAL binding to two symmetrical sites formed by the TLR TIR dimer, and was supported by extensive mutagenesis studies, phosphorylation site analysis, and peptide inhibition mapping [106]. In contrast, on the basis of a crystallographic structure of a homodimeric bacterial TIR domain which interferes with MyD88 function, its BB loop was proposed to play a role not in homotypic TIR interactions but in heterotypic interactions with MyD88, further highlighting the diversity of possible protein-protein interfaces associated with TIR domain assemblies.

Finally, it should be noted that a significant body of recent evidence indicates that the engagement of adaptor proteins with the TIR domains of TLRs results in the assembly of extensive higher-order macromolecular complexes that promote downstream immune responses, and may be important in TLR-dependent clustering and signal amplification [99]. The best characterized one, termed the "Myddosome", results in MyD88-dependent activation of NF-κB activation [108]. By analogy, oligomeric TRIF-based complexes ("Triffosome") are also known to exist, though their structural characterization is less far advanced [21]. MyD88 contains two signalling domains, an amino-terminal TIR domain, and a carboxy-terminal death domain which can recruit IL-1R-associated kinase (IRAK) proteins via their own death domains, thus stimulating kinase activity. The crystal structure of a complex formed by the death domains of MyD88, IRAK4, and IRAK2 [111] provided insights into at least one form of the Myddosome. The large complex consisted of a helical, three-layered arrangement of six MyD88, four IRAK-4, and four IRAK-2 death domains. This layered arrangement is suggestive of the sequential process of recruitment that may enable positive cooperativity in signalling. This complex may be important in higher-order clustering of TLRs by interacting with additional TLR dimers, and there is evidence that the Myddosome complex stoichiometry varies *in vivo*, which may result in differential signalling outputs [21].

CONCLUSIONS

A large body of high-resolution crystallographic data is now available for the ectodomains of homo- and heterodimeric TLR and TLR-like complexes, highlighting general themes and key differences across the family. Moreover, recent structural information, supported by a wealth of biochemical and simulation data, has provided insights into the mechanisms by which these ectodomains and associated co-receptor proteins propagate allosteric signals across protein-protein interfaces to determine the formation and stability of

productive receptor complexes. Furthermore, recent structural data combined with computational modeling have provided new insights into the possible protein-protein interactions involved in TLR transmembrane assembly and TIR-mediated signaling complex formation. Nevertheless, our understanding of TLR function would benefit from further structural information concerning modes of interaction and oligomerization, particularly in the context of the physiologically-relevant environment. For example, the stability of several TLR complexes and their interaction with ligands are dependent upon local pH, whilst the lipid membrane in which TLRs are embedded are likely to influence both TM structure/dynamics and the interaction with membrane proximal adaptor proteins and associated complexes. Likewise, higher-order macromolecular assembly beyond the TLR dimer may be relevant in a biological setting, and combined with receptor clustering (possibly in a lipid raft dependent manner) [99], likely plays a key role in determining receptor cooperativity and hence the cellular signalling output. Further structural, biochemical, and computational studies should continue to uncover new insights into the interplay between the different TLR components, and ultimately drive the development of novel therapeutic approaches to inflammatory diseases and sepsis.

ACKNOWLEDGEMENTS

We thank the A*STAR Graduate Academy (A*GA) Singapore for funding.

TABLES

Table 1. Structural and functional properties of ligand-bound TLR dimers.

TLR Homo- or Hetero-Dimer	Species	PDB code	LRRs per Ecto-domain	LRRs Directly Involved in TLR-TLR Interface	Bound Ligand	Location	TLR / TLR Buried Area (Å²) *
TLR1-TLR2	Human	2Z7X [10]	20	11-14	Tri-acylated lipopeptides	Cell surface	~690
TLR2-TLR6	Mouse	3A79 [11]	20	11-14	Di-acylated lipopeptides	Cell surface	~655
TLR3-TLR3	Mouse	3CIY [89]	25	20	dsRNA	Endosomal	~435
TLR4-TLR4	Human	3FXI [57]	23	13, 15, 17, 20	Lipid A	Cell surface & Endosomal	~465
TLR5-TLR5	Zebrafish	3V47 [43]	22	12-13	Flagellin	Cell surface	~735
TLR7-TLR7	N/A	N/A	27	N/A	ssRNA	Endosomal	N/A
TLR8-TLR8	Human	4QBZ [14]	27	5, 8, 14-20	ssRNA	Endosomal	~2000
TLR9-TLR9	Horse	3WPC [19]	27	2, 5, 8, 11, 18, 20-25	CpG DNA	Endosomal	~2250
TLR10-TLR10	N/A	N/A	20	N/A	Unknown but see Lee *et al* [41]	Cell surface	N/A

* buried surface area calculated using GROMACS analysis tools (http://www.gromacs.org/).

FIGURE LEGENDS

Figure 1. Crystal structures of TLR ectodomains with both ligands. Structures are shown for: **(A)** the TLR1-2 heterodimer in complex with Pam_3CSK_4 (PDB:2Z7X); **(B)** the TLR2-TLR6 heterodimer in complex with Pam_2CSK_4 (PDB:3A79); **(C)** the TLR3 homodimer in complex with dsRNA (PDB:3CIY); **(D)** the TLR4/MD-2 heterotetramer in complex with LPS (PDB:3FXI); **(E)** the TLR5 homodimer in complex with flagellin (PDB:3V47); **(F)** the TLR8 homodimer in complex with a nucleoside (PDB:4QBZ); and **(G)** the TLR9 homodimer in complex with ssDNA (PDB:3WPC). The individual TLR chains in each dimer are shown as blue and yellow cartoons, with ligand in green wireframe format. Bound MD-2 co-receptor for TLR4 is shown in red cartoons format. The carboxy-termini are indicated by labels (CT) in each TLR ectodomain structure.

Figure 2. Conformational changes in the carboxy-terminal regions of TLR ectodomains, which may be related to downstream signaling. Crystal structures are shown for TLR8 in **(A)** the ligand-bound state (PDB:4QBZ) and **(B)** the ligand-free state (PDB:3W3G). In **(C)**, the TLR4 ectodomain dimer from the crystal structure of the TLR4/MD-2 complex bound to LPS ligand (PDB:3FXI) is shown, and compared with **(D)** porcupine plot representing simulated dominant motions of the TLR4 ectodomain dimer, with magnitudes of atomic motion indicated by length and color of associated arrows. In the TLR8 crystal structures, the ectodomain chains are represented as cartoons, with the ligand in red wireframe format. For clarity, only the ectodomain chains are shown for the TLR4 crystal structure, in cartoons format. The porcupine plot is based on molecular dynamics simulations of TLR4 in the absence of bound ligand (48), derived from principal components analysis of the trajectory.

Figure 3. The molecular switch in TLR4 signaling. Snapshots derived from molecular dynamics simulations (48), are shown for the TLR4/MD-2 heterotetrameric complex in **(A)** the presence of bound lipid A, and **(B)** the ligand-free, apo state. The two TLR4 chains are shown as blue and yellow cartoons, with an MD-2 co-receptor in red cartoons format, and bound ligand is shown in green wireframe representation. The key Phe126 residue that switches between the ligand-bound and free states, thus influencing the stability of the complex, is shown in CPK spacefill format.

Figure 4. The RP105/MD-1 complex that inhibits TRL4 function. In **(A)** the crystal structure of RP105 (PDB:3RG1) in the heterotetrameric $(RP105/MD\text{-}1)_2$ complex is shown. In **(B)** a hypothetical inhibitory model of the RP105/TLR4 complex is shown, modeled using PDB structures 3B2D (RP105) and 3FXI (TLR4), and based on work by Yoon *et al* (72). The carboxy-termini are indicated by labels (CT) for each RP105 and TLR ectodomain structure. Each protein chain is shown in cartoons format, with ligand (TLR4) or oligosaccharide (RP105) colored in green wireframe format. RP105 chains are shown in cyan and grey, with MD-1 in mauve. TLR4 chains are colored in blue and yellow, with MD-2 in red.

Figure 5: The structure and dynamics of transmembrane TLR3 domains. In **(A)** the structure of the lowest-energy solution NMR model of the TM domain of dimeric TLR3 within DPC micelles is shown. This was used to setup a molecular dynamics simulation system, shown in **(B)**, containing the TLR3 transmembrane dimer, rotated by 90° about its axis compared to (A), embedded within a POPC lipid bilayer and solvated by a physiological salt solution. In **(C)**, the final, equilibrated structure from this simulation is shown, from the same perspective as (A). The transmembrane helices are shown as cartoons, with sidechains key to stability of the dimeric interface represented in wireframe format and labelled. In the simulation system snapshot, phospholipids and water are shown in CPK spacefill representation.

REFERENCES

1. Mogensen TH (2009) Pathogen recognition and inflammatory signaling in innate immune defenses. Clin Microbiol Rev 22: 240-273, Table of Contents.
2. Kumar H, Kawai T, Akira S (2011) Pathogen recognition by the innate immune system. Int Rev Immunol 30: 16-34.
3. Janeway CA, Jr. (1989) Approaching the asymptote? Evolution and revolution in immunology. Cold Spring Harb Symp Quant Biol 54 Pt 1: 1-13.
4. Medzhitov R, Preston-Hurlburt P, Janeway CA, Jr. (1997) A human homologue of the Drosophila Toll protein signals activation of adaptive immunity. Nature 388: 394-397.
5. Fink A, Reuven EM, Arnusch CJ, Shmuel-Galia L, Antonovsky N, et al. (2013) Assembly of the TLR2/6 transmembrane domains is essential for activation and is a target for prevention of sepsis. J Immunol 190: 6410-6422.
6. Roger T, Froidevaux C, Le Roy D, Reymond MK, Chanson AL, et al. (2009) Protection from lethal gram-negative bacterial sepsis by targeting Toll-like receptor 4. Proc Natl Acad Sci U S A 106: 2348-2352.
7. Savva A, Roger T (2013) Targeting toll-like receptors: promising therapeutic strategies for the management of sepsis-associated pathology and infectious diseases. Front Immunol 4: 387.
8. Wittebole X, Castanares-Zapatero D, Laterre PF (2010) Toll-like receptor 4 modulation as a strategy to treat sepsis. Mediators Inflamm 2010: 568396.
9. O'Neill LA, Bryant CE, Doyle SL (2009) Therapeutic targeting of Toll-like receptors for infectious and inflammatory diseases and cancer. Pharmacol Rev 61: 177-197.
10. Jin MS, Kim SE, Heo JY, Lee ME, Kim HM, et al. (2007) Crystal structure of the TLR1-TLR2 heterodimer induced by binding of a tri-acylated lipopeptide. Cell 130: 1071-1082.
11. Kang JY, Nan X, Jin MS, Youn SJ, Ryu YH, et al. (2009) Recognition of lipopeptide patterns by Toll-like receptor 2-Toll-like receptor 6 heterodimer. Immunity 31: 873-884.
12. Kim HM, Park BS, Kim JI, Kim SE, Lee J, et al. (2007) Crystal structure of the TLR4-MD-2 complex with bound endotoxin antagonist Eritoran. Cell 130: 906-917.
13. Bell JK, Botos I, Hall PR, Askins J, Shiloach J, et al. (2006) The molecular structure of the TLR3 extracellular domain. J Endotoxin Res 12: 375-378.
14. Yoo E, Salunke DB, Sil D, Guo X, Salyer AC, et al. (2014) Determinants of activity at human Toll-like receptors 7 and 8: quantitative structure-activity relationship (QSAR) of diverse heterocyclic scaffolds. J Med Chem 57: 7955-7970.
15. Wei T, Gong J, Jamitzky F, Heckl WM, Stark RW, et al. (2009) Homology modeling of human Toll-like receptors TLR7, 8, and 9 ligand-binding domains. Protein Sci 18: 1684-1691.
16. Ohto U, Tanji H, Shimizu T (2014) Structure and function of toll-like receptor 8. Microbes Infect 16: 273-282.

17. Choe J, Kelker MS, Wilson IA (2005) Crystal structure of human toll-like receptor 3 (TLR3) ectodomain. Science 309: 581-585.
18. Tanji H, Ohto U, Shibata T, Miyake K, Shimizu T (2013) Structural reorganization of the Toll-like receptor 8 dimer induced by agonistic ligands. Science 339: 1426-1429.
19. Ohto U, Shibata T, Tanji H, Ishida H, Krayukhina E, et al. (2015) Structural basis of CpG and inhibitory DNA recognition by Toll-like receptor 9. Nature 520: 702-705.
20. Akira S, Takeda K (2004) Toll-like receptor signalling. Nat Rev Immunol 4: 499-511.
21. Gay NJ, Symmons MF, Gangloff M, Bryant CE (2014) Assembly and localization of Toll-like receptor signalling complexes. Nat Rev Immunol 14: 546-558.
22. Reuven EM, Fink A, Shai Y (2014) Regulation of innate immune responses by transmembrane interactions: lessons from the TLR family. Biochim Biophys Acta 1838: 1586-1593.
23. Yamamoto M, Takeda K (2010) Current views of toll-like receptor signaling pathways. Gastroenterol Res Pract 2010: 240365.
24. Gautam JK, Ashish, Comeau LD, Krueger JK, Smith MF, Jr. (2006) Structural and functional evidence for the role of the TLR2 DD loop in TLR1/TLR2 heterodimerization and signaling. J Biol Chem 281: 30132-30142.
25. Roach JC, Glusman G, Rowen L, Kaur A, Purcell MK, et al. (2005) The evolution of vertebrate Toll-like receptors. Proc Natl Acad Sci U S A 102: 9577-9582.
26. Buchanan SG, Gay NJ (1996) Structural and functional diversity in the leucine-rich repeat family of proteins. Prog Biophys Mol Biol 65: 1-44.
27. Enkhbayar P, Kamiya M, Osaki M, Matsumoto T, Matsushima N (2004) Structural principles of leucine-rich repeat (LRR) proteins. Proteins 54: 394-403.
28. Gay NJ, Gangloff M (2007) Structure and function of Toll receptors and their ligands. Annu Rev Biochem 76: 141-165.
29. Kajava AV (1998) Structural diversity of leucine-rich repeat proteins. J Mol Biol 277: 519-527.
30. Kobe B, Kajava AV (2001) The leucine-rich repeat as a protein recognition motif. Curr Opin Struct Biol 11: 725-732.
31. Bella J, Hindle KL, McEwan PA, Lovell SC (2008) The leucine-rich repeat structure. Cell Mol Life Sci 65: 2307-2333.
32. Kang JY, Lee JO (2011) Structural biology of the Toll-like receptor family. Annu Rev Biochem 80: 917-941.
33. Matsushima N, Tanaka T, Enkhbayar P, Mikami T, Taga M, et al. (2007) Comparative sequence analysis of leucine-rich repeats (LRRs) within vertebrate toll-like receptors. BMC Genomics 8: 124.
34. Manukyan M, Triantafilou K, Triantafilou M, Mackie A, Nilsen N, et al. (2005) Binding of lipopeptide to CD14 induces physical proximity of CD14, TLR2 and TLR1. Eur J Immunol 35: 911-921.
35. Shimizu T, Kida Y, Kuwano K (2008) A triacylated lipoprotein from Mycoplasma genitalium activates NF-kappaB through Toll-like receptor 1 (TLR1) and TLR2. Infect Immun 76: 3672-3678.

36. Omueti KO, Mazur DJ, Thompson KS, Lyle EA, Tapping RI (2007) The polymorphism P315L of human toll-like receptor 1 impairs innate immune sensing of microbial cell wall components. J Immunol 178: 6387-6394.
37. Grabiec A, Meng G, Fichte S, Bessler W, Wagner H, et al. (2004) Human but not murine toll-like receptor 2 discriminates between tri-palmitoylated and tri-lauroylated peptides. J Biol Chem 279: 48004-48012.
38. Irvine KL, Hopkins LJ, Gangloff M, Bryant CE (2013) The molecular basis for recognition of bacterial ligands at equine TLR2, TLR1 and TLR6. Vet Res 44: 50.
39. Farhat K, Riekenberg S, Heine H, Debarry J, Lang R, et al. (2008) Heterodimerization of TLR2 with TLR1 or TLR6 expands the ligand spectrum but does not lead to differential signaling. J Leukoc Biol 83: 692-701.
40. Guan Y, Ranoa DR, Jiang S, Mutha SK, Li X, et al. (2010) Human TLRs 10 and 1 share common mechanisms of innate immune sensing but not signaling. J Immunol 184: 5094-5103.
41. Lee SM, Kok KH, Jaume M, Cheung TK, Yip TF, et al. (2014) Toll-like receptor 10 is involved in induction of innate immune responses to influenza virus infection. Proc Natl Acad Sci U S A 111: 3793-3798.
42. Smith KD, Andersen-Nissen E, Hayashi F, Strobe K, Bergman MA, et al. (2003) Toll-like receptor 5 recognizes a conserved site on flagellin required for protofilament formation and bacterial motility. Nat Immunol 4: 1247-1253.
43. Yoon SI, Kurnasov O, Natarajan V, Hong M, Gudkov AV, et al. (2012) Structural basis of TLR5-flagellin recognition and signaling. Science 335: 859-864.
44. Zhou K, Kanai R, Lee P, Wang HW, Modis Y (2012) Toll-like receptor 5 forms asymmetric dimers in the absence of flagellin. J Struct Biol 177: 402-409.
45. Miao EA, Andersen-Nissen E, Warren SE, Aderem A (2007) TLR5 and Ipaf: dual sensors of bacterial flagellin in the innate immune system. Semin Immunopathol 29: 275-288.
46. Andersen-Nissen E, Smith KD, Bonneau R, Strong RK, Aderem A (2007) A conserved surface on Toll-like receptor 5 recognizes bacterial flagellin. J Exp Med 204: 393-403.
47. Gangloff M (2012) Different dimerisation mode for TLR4 upon endosomal acidification? Trends Biochem Sci 37: 92-98.
48. Paramo T, Piggot TJ, Bryant CE, Bond PJ (2013) The structural basis for endotoxin-induced allosteric regulation of the Toll-like receptor 4 (TLR4) innate immune receptor. J Biol Chem 288: 36215-36225.
49. Park BS, Lee JO (2013) Recognition of lipopolysaccharide pattern by TLR4 complexes. Exp Mol Med 45: e66.
50. Resman N, Vasl J, Oblak A, Pristovsek P, Gioannini TL, et al. (2009) Essential roles of hydrophobic residues in both MD-2 and toll-like receptor 4 in activation by endotoxin. J Biol Chem 284: 15052-15060.
51. Scior T, Alexander C, Zaehringer U (2013) Reviewing and identifying amino acids of human, murine, canine and equine TLR4 / MD-2 receptor complexes conferring endotoxic innate immunity activation by LPS/lipid

A, or antagonistic effects by Eritoran, in contrast to species-dependent modulation by lipid IVa. Comput Struct Biotechnol J 5: e201302012.
52. Walsh C, Gangloff M, Monie T, Smyth T, Wei B, et al. (2008) Elucidation of the MD-2/TLR4 interface required for signaling by lipid IVa. J Immunol 181: 1245-1254.
53. Yu L, Phillips RL, Zhang D, Teghanemt A, Weiss JP, et al. (2012) NMR studies of hexaacylated endotoxin bound to wild-type and F126A mutant MD-2 and MD-2.TLR4 ectodomain complexes. J Biol Chem 287: 16346-16355.
54. Romero CD, Varma TK, Hobbs JB, Reyes A, Driver B, et al. (2011) The Toll-like receptor 4 agonist monophosphoryl lipid a augments innate host resistance to systemic bacterial infection. Infect Immun 79: 3576-3587.
55. Erridge C, Bennett-Guerrero E, Poxton IR (2002) Structure and function of lipopolysaccharides. Microbes Infect 4: 837-851.
56. Bryant CE, Spring DR, Gangloff M, Gay NJ (2010) The molecular basis of the host response to lipopolysaccharide. Nat Rev Microbiol 8: 8-14.
57. Park BS, Song DH, Kim HM, Choi BS, Lee H, et al. (2009) The structural basis of lipopolysaccharide recognition by the TLR4-MD-2 complex. Nature 458: 1191-1195.
58. Ohto U, Fukase K, Miyake K, Satow Y (2007) Crystal structures of human MD-2 and its complex with antiendotoxic lipid IVa. Science 316: 1632-1634.
59. Netea MG, van Deuren M, Kullberg BJ, Cavaillon JM, Van der Meer JW (2002) Does the shape of lipid A determine the interaction of LPS with Toll-like receptors? Trends Immunol 23: 135-139.
60. Saitoh S, Akashi S, Yamada T, Tanimura N, Kobayashi M, et al. (2004) Lipid A antagonist, lipid IVa, is distinct from lipid A in interaction with Toll-like receptor 4 (TLR4)-MD-2 and ligand-induced TLR4 oligomerization. Int Immunol 16: 961-969.
61. Talbot S, Totemeyer S, Yamamoto M, Akira S, Hughes K, et al. (2009) Toll-like receptor 4 signalling through MyD88 is essential to control Salmonella enterica serovar typhimurium infection, but not for the initiation of bacterial clearance. Immunology 128: 472-483.
62. Paramo T, East A, Garzon D, Ulmschneider MB, Bond PJ (2014) Efficient Characterization of Protein Cavities within Molecular Simulation Trajectories: trj_cavity. J Chem Theory Comput 10: 2151-2164.
63. Miura Y, Shimazu R, Miyake K, Akashi S, Ogata H, et al. (1998) RP105 is associated with MD-1 and transmits an activation signal in human B cells. Blood 92: 2815-2822.
64. Miyake K, Shimazu R, Kondo J, Niki T, Akashi S, et al. (1998) Mouse MD-1, a molecule that is physically associated with RP105 and positively regulates its expression. J Immunol 161: 1348-1353.
65. Nagai Y, Shimazu R, Ogata H, Akashi S, Sudo K, et al. (2002) Requirement for MD-1 in cell surface expression of RP105/CD180 and B-cell responsiveness to lipopolysaccharide. Blood 99: 1699-1705.
66. Blumenthal A, Kobayashi T, Pierini LM, Banaei N, Ernst JD, et al. (2009) RP105 facilitates macrophage activation by Mycobacterium tuberculosis lipoproteins. Cell Host Microbe 5: 35-46.
67. Miyake K, Yamashita Y, Hitoshi Y, Takatsu K, Kimoto M (1994) Murine B cell proliferation and protection from apoptosis with an antibody against a

105-kD molecule: unresponsiveness of X-linked immunodeficient B cells. J Exp Med 180: 1217-1224.
68. Yamashita Y, Miyake K, Miura Y, Kaneko Y, Yagita H, et al. (1996) Activation mediated by RP105 but not CD40 makes normal B cells susceptible to anti-IgM-induced apoptosis: a role for Fc receptor coligation. J Exp Med 184: 113-120.
69. Nagai Y, Yanagibashi T, Watanabe Y, Ikutani M, Kariyone A, et al. (2012) The RP105/MD-1 complex is indispensable for TLR4/MD-2-dependent proliferation and IgM-secreting plasma cell differentiation of marginal zone B cells. Int Immunol 24: 389-400.
70. Chaplin JW, Kasahara S, Clark EA, Ledbetter JA (2011) Anti-CD180 (RP105) activates B cells to rapidly produce polyclonal Ig via a T cell and MyD88-independent pathway. J Immunol 187: 4199-4209.
71. Ohto U, Miyake K, Shimizu T (2011) Crystal structures of mouse and human RP105/MD-1 complexes reveal unique dimer organization of the toll-like receptor family. J Mol Biol 413: 815-825.
72. Yoon SI, Hong M, Wilson IA (2011) An unusual dimeric structure and assembly for TLR4 regulator RP105-MD-1. Nat Struct Mol Biol 18: 1028-1035.
73. Divanovic S, Trompette A, Atabani SF, Madan R, Golenbock DT, et al. (2005) Negative regulation of Toll-like receptor 4 signaling by the Toll-like receptor homolog RP105. Nat Immunol 6: 571-578.
74. Divanovic S, Trompette A, Petiniot LK, Allen JL, Flick LM, et al. (2007) Regulation of TLR4 signaling and the host interface with pathogens and danger: the role of RP105. J Leukoc Biol 82: 265-271.
75. Godfroy JI, 3rd, Roostan M, Moroz YS, Korendovych IV, Yin H (2012) Isolated Toll-like receptor transmembrane domains are capable of oligomerization. PLoS One 7: e48875.
76. Shai Y (1995) Molecular recognition between membrane-spanning polypeptides. Trends Biochem Sci 20: 460-464.
77. Mendrola JM, Berger MB, King MC, Lemmon MA (2002) The single transmembrane domains of ErbB receptors self-associate in cell membranes. J Biol Chem 277: 4704-4712.
78. Zhu H, Metcalf DG, Streu CN, Billings PC, Degrado WF, et al. (2010) Specificity for homooligomer versus heterooligomer formation in integrin transmembrane helices. J Mol Biol 401: 882-891.
79. Finger C, Escher C, Schneider D (2009) The single transmembrane domains of human receptor tyrosine kinases encode self-interactions. Sci Signal 2: ra56.
80. Nemoto W, Toh H (2006) Membrane interactive alpha-helices in GPCRs as a novel drug target. Curr Protein Pept Sci 7: 561-575.
81. Zhang H, Tay PN, Cao W, Li W, Lu J (2002) Integrin-nucleated Toll-like receptor (TLR) dimerization reveals subcellular targeting of TLRs and distinct mechanisms of TLR4 activation and signaling. FEBS Lett 532: 171-176.
82. Treeby M, Vasl J, Ota P, Friedrich J, Jerala R (2009) Different functional role of domain boundaries of Toll-like receptor 4. Biochem Biophys Res Commun 381: 65-69.

83. Panter G, Jerala R (2011) The ectodomain of the Toll-like receptor 4 prevents constitutive receptor activation. J Biol Chem 286: 23334-23344.
84. Latz E, Verma A, Visintin A, Gong M, Sirois CM, et al. (2007) Ligand-induced conformational changes allosterically activate Toll-like receptor 9. Nat Immunol 8: 772-779.
85. Miller VL, Taylor RK, Mekalanos JJ (1987) Cholera toxin transcriptional activator toxR is a transmembrane DNA binding protein. Cell 48: 271-279.
86. Langosch D, Brosig B, Kolmar H, Fritz HJ (1996) Dimerisation of the glycophorin A transmembrane segment in membranes probed with the ToxR transcription activator. J Mol Biol 263: 525-530.
87. Lindner E, Langosch D (2006) A ToxR-based dominant-negative system to investigate heterotypic transmembrane domain interactions. Proteins 65: 803-807.
88. Mineev KS, Goncharuk SA, Arseniev AS (2014) Toll-like receptor 3 transmembrane domain is able to perform various homotypic interactions: an NMR structural study. FEBS Lett 588: 3802-3807.
89. Liu L, Botos I, Wang Y, Leonard JN, Shiloach J, et al. (2008) Structural basis of toll-like receptor 3 signaling with double-stranded RNA. Science 320: 379-381.
90. Heyda J, Mason PE, Jungwirth P (2010) Attractive interactions between side chains of histidine-histidine and histidine-arginine-based cationic dipeptides in water. J Phys Chem B 114: 8744-8749.
91. Mineev KS, Khabibullina NF, Lyukmanova EN, Dolgikh DA, Kirpichnikov MP, et al. (2011) Spatial structure and dimer--monomer equilibrium of the ErbB3 transmembrane domain in DPC micelles. Biochim Biophys Acta 1808: 2081-2088.
92. Bocharov EV, Mineev KS, Goncharuk MV, Arseniev AS (2012) Structural and thermodynamic insight into the process of "weak" dimerization of the ErbB4 transmembrane domain by solution NMR. Biochim Biophys Acta 1818: 2158-2170.
93. Fisher LE, Engelman DM, Sturgis JN (1999) Detergents modulate dimerization, but not helicity, of the glycophorin A transmembrane domain. J Mol Biol 293: 639-651.
94. Fleming KG (2002) Standardizing the free energy change of transmembrane helix-helix interactions. J Mol Biol 323: 563-571.
95. MacKenzie KR, Prestegard JH, Engelman DM (1997) A transmembrane helix dimer: structure and implications. Science 276: 131-133.
96. Smith SO, Song D, Shekar S, Groesbeek M, Ziliox M, et al. (2001) Structure of the transmembrane dimer interface of glycophorin A in membrane bilayers. Biochemistry 40: 6553-6558.
97. Cuthbertson JM, Bond PJ, Sansom MS (2006) Transmembrane helix-helix interactions: comparative simulations of the glycophorin a dimer. Biochemistry 45: 14298-14310.
98. Bond PJ, Sansom MS (2006) Insertion and assembly of membrane proteins via simulation. J Am Chem Soc 128: 2697-2704.
99. Bryant CE, Symmons M, Gay NJ (2015) Toll-like receptor signalling through macromolecular protein complexes. Mol Immunol 63: 162-165.

100. Jang TH, Park HH (2014) Crystal structure of TIR domain of TLR6 reveals novel dimeric interface of TIR-TIR interaction for toll-like receptor signaling pathway. J Mol Biol 426: 3305-3313.
101. Nyman T, Stenmark P, Flodin S, Johansson I, Hammarstrom M, et al. (2008) The crystal structure of the human toll-like receptor 10 cytoplasmic domain reveals a putative signaling dimer. J Biol Chem 283: 11861-11865.
102. Xu Y, Tao X, Shen B, Horng T, Medzhitov R, et al. (2000) Structural basis for signal transduction by the Toll/interleukin-1 receptor domains. Nature 408: 111-115.
103. Hasan U, Chaffois C, Gaillard C, Saulnier V, Merck E, et al. (2005) Human TLR10 is a functional receptor, expressed by B cells and plasmacytoid dendritic cells, which activates gene transcription through MyD88. J Immunol 174: 2942-2950.
104. Poltorak A, He X, Smirnova I, Liu MY, Van Huffel C, et al. (1998) Defective LPS signaling in C3H/HeJ and C57BL/10ScCr mice: mutations in Tlr4 gene. Science 282: 2085-2088.
105. Verstak B, Arnot CJ, Gay NJ (2013) An alanine-to-proline mutation in the BB-loop of TLR3 Toll/IL-1R domain switches signalling adaptor specificity from TRIF to MyD88. J Immunol 191: 6101-6109.
106. Nunez Miguel R, Wong J, Westoll JF, Brooks HJ, O'Neill LA, et al. (2007) A dimer of the Toll-like receptor 4 cytoplasmic domain provides a specific scaffold for the recruitment of signalling adaptor proteins. PLoS One 2: e788.
107. Toshchakov VY, Fenton MJ, Vogel SN (2007) Cutting Edge: Differential inhibition of TLR signaling pathways by cell-permeable peptides representing BB loops of TLRs. J Immunol 178: 2655-2660.
108. Anwar MA, Basith S, Choi S (2013) Negative regulatory approaches to the attenuation of Toll-like receptor signaling. Exp Mol Med 45: e11.
109. Basith S, Manavalan B, Govindaraj RG, Choi S (2011) In silico approach to inhibition of signaling pathways of Toll-like receptors 2 and 4 by ST2L. PLoS One 6: e23989.
110. Tao X, Xu Y, Zheng Y, Beg AA, Tong L (2002) An extensively associated dimer in the structure of the C713S mutant of the TIR domain of human TLR2. Biochem Biophys Res Commun 299: 216-221.
111. Lin SC, Lo YC, Wu H (2010) Helical assembly in the MyD88-IRAK4-IRAK2 complex in TLR/IL-1R signalling. Nature 465: 885-890.

FIGURE 1

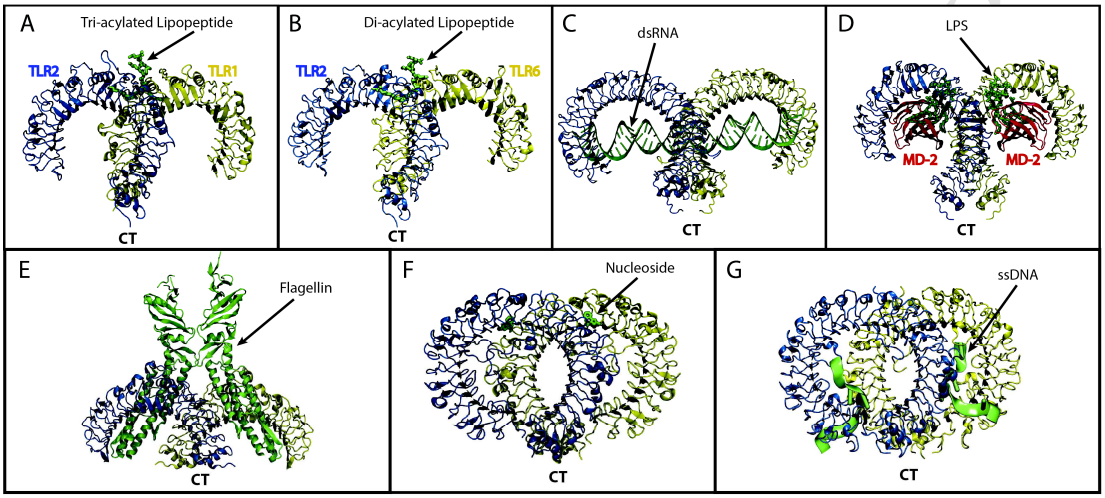

FIGURE 2

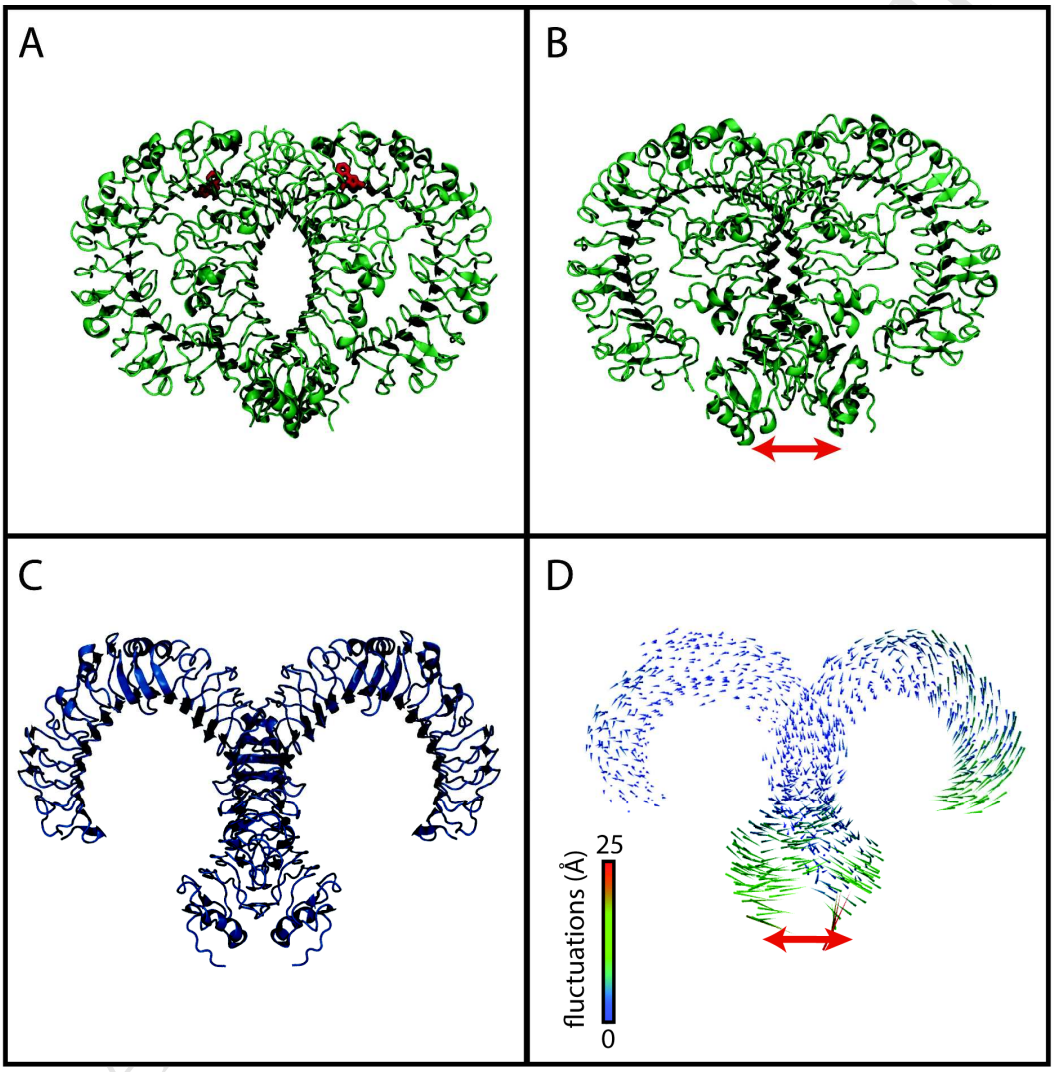

FIGURE 3

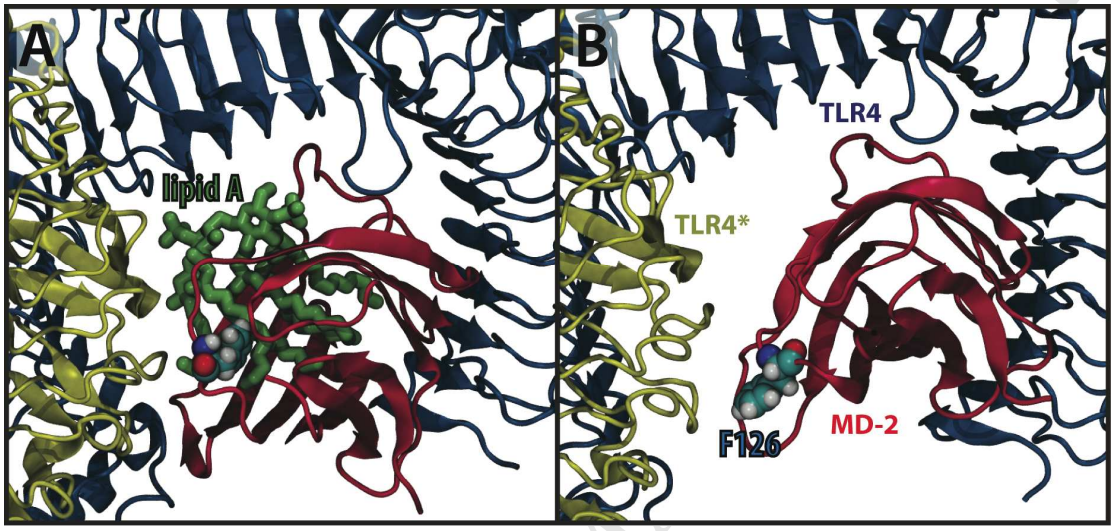

FIGURE 4

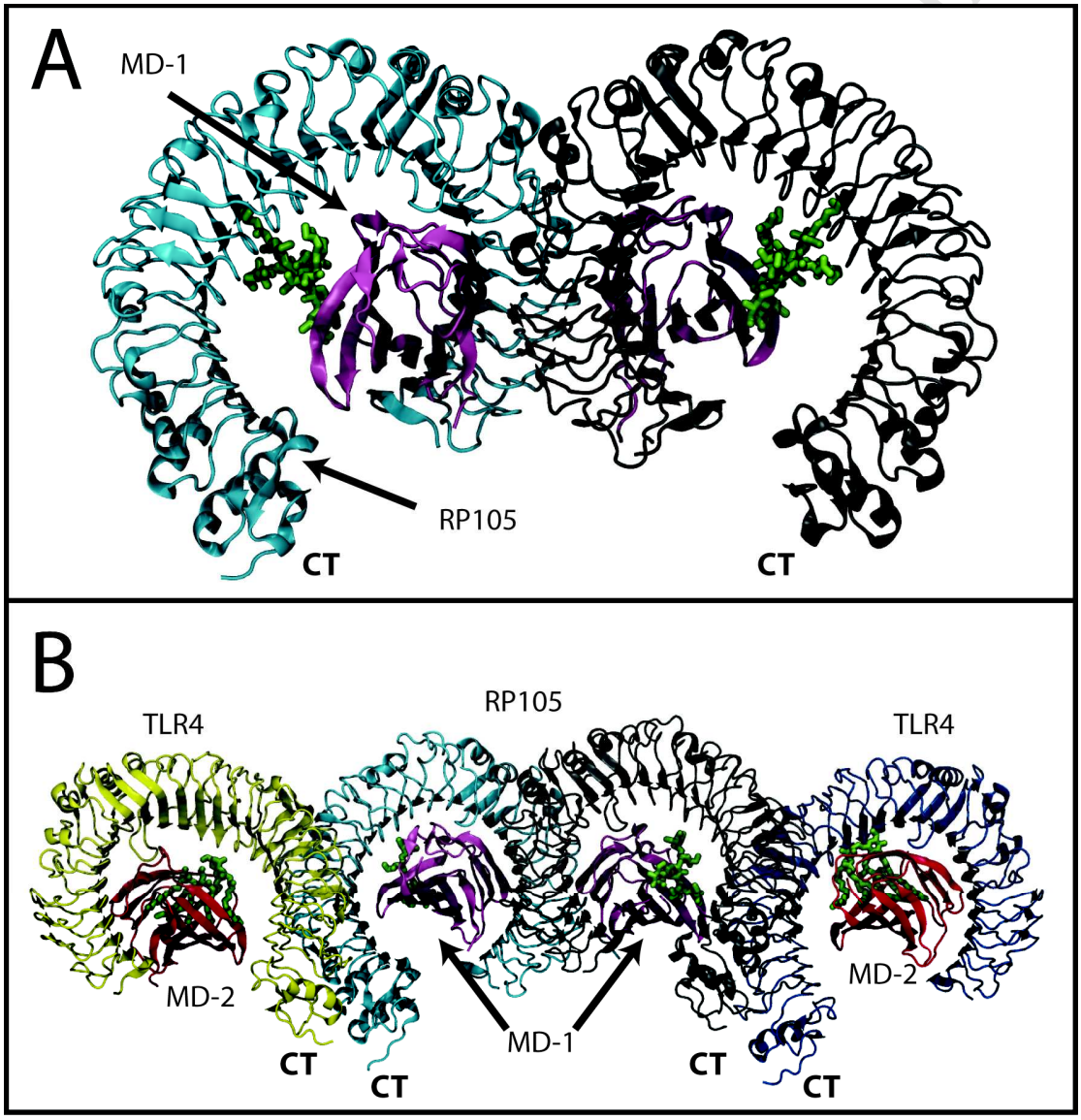

FIGURE 5